Comparison of two methods for the Young´s Modulus determination of thin silicon nitride films: Cantilever bending and instrumented indentation technique in the mirco and nano range

N. Wollschläger[a*], P. Reinstädt[b], W. Österle[a], M. Griepentrog[b]

[a] BAM Federal Institute of Materials Research and Testing, Division of Materialography, Fractography and Aging of Engineering Materials, Unter den Eichen 87, 12205 Berlin, Germany

[b] BAM Federal Institute of Materials Research and Testing, Division of Surface Modification and Measurement Technique, Fabeckstraße 60-62, 12203 Berlin, Germany

* Corresponding author. Tel.: +49 03 8104 4712. E-mail address: nicole.wollschlaeger@bam.de

Submission to: Thin solid films

Abstract

Mechanical testing on nano-objects or thin films is still a challenging task retrieving a lot of sources of error which can have an enormous influence on the final result. Here two methods were carried out on 50 nm, 100 nm, 200 nm and 500 nm thin silicon nitride films to determine the elastic properties and to check for a possible size effect. The first method involved bending of as-prepared free-standing beams with a cantilever-based force measurement tool mounted in the vacuum chamber of a scanning electron microscope. The second method was based on nanoindentation on the the same films, although still adhering to their silicon substrates, following the ISO standard procedure 14577. The aim here was to compare the results of both methods. For the bending method Young´s Moduli of about (205 ± 10) GPa

were obtained, for nanoindentation values amount to (254 ± 20) GPa. A size effect was not observed and both values are in agreement with the literature. Nevertheless, there is a mismatch between the results due to the uncertainties and difficulties in each technique. These were critically examined by listing and evaluating the error sources in detail. Especially it is demonstrated which parameters have to be known exactly and what is happening if small deviations are taken into account. At the end the comparability of these techniques is checked with regard to the fact that both methods base on completely different models and simplifications. Out of this knowledge recommendations can be derived for testing at the nanoscale using either bending or nanoindentation.

Keywords: mechanical properties, Young´s Modulus, bending, nanoindentation, thin films, uncertainty budget, silicon nitride

1. Introduction

Structural elements become smaller and smaller with the progressing technical evolution. The advantages are on hand: saving material and lowering costs for the preparation. Typical application fields of mirco- and nano-mechanical systems in combination with nano-objects or membranes are medicine or analytical science and technology [1-5]. Other industrial issues deal with scratch-resistant and shockproof thin coatings in the sub-micron range [6-9]. All of these components shall exhibit certain mechanical properties concerning their flexibility or fracture toughness. This has to be checked also in the context of an assumed size effect, predicting higher bending strength for smaller volumes where the probability of critical flaws is smaller [10]. Measuring the mechanical properties of such nano- and micro-objects or films is a challenging task retrieving lot of sources of error. There are various techniques on the

market such as indentation [11-13], tensile testing [14], bending [15-20] and resonance tests [21], just to mention some of them. But often the results are not comparable, sources of error are hardly considered and the influence of the preparation is not clear in all cases. Therefore it is still interesting to determine material properties at the nanoscale and have a detailed critical look on them. Furthermore, there is a need to improve measuring methods and to develop new techniques.

In this publication the scope is on the detailed comparison of two different methods for the determination of the Young´s Modulus. The first method is based on in-situ bending tests on as-prepared beam-like objects with a micromanipulator equipped with a force measurement tool (see Fig. 2a). The objects were cut out of commercially available free-standing silicon nitride membranes by the Focused Ion Beam (FIB) technique. The applied force measurement technique is less investigated, but the set-up is simple and sources of error exist in a manageable amount. Only few parameters have to be checked for the determination of the Young´s Modulus: The correct force and displacement detection and the geometry parameters of the as-prepared beam-like nanostructure. Especially for brittle materials as silicon nitride the bending test is a suitable method in comparison to tensile testing, where no or less information about the deformation capability are available out of the measuring set-up. In a bending test this information can be extracted easily by the detection of the displacement.

Additionally, the same thin films adhered to the bulk silicon wafer were tested using the established instrumented indentation technique (IIT) as a second different method. The measurement of the Young's Modulus of thin films using IIT, commonly known also as nanoindentation, is still challenging, because nanoindentation is very sensitive to surface roughness and inhomogeneity of the tested material. Another important point relates to the influence of the substrate on the measured value of the modulus, which increases with increasing modulus ratio between film and substrate. Even for small ratios of indentation depth to film thickness the measured indentation modulus for the film is still affected by the

substrate. Several approaches to calculate the film modulus can be found in the literature. For example Bhattachary and Nix [22] were using finite elements (FE) modeling for a rigid conical indenter and silicon and aluminum as substrate and film materials. Another possibility was shown by Chudoba et al. These authors found an analytical solution for the Hertzian contact of coated systems in combination with a spherical indenter to calculate the modulus on ultra-thin-coatings [23]. The method, for the IIT data, used in this article to calculate the Young's Modulus of the silicon nitride films is based on the concept of an "effective indenter shape" first introduced by Pharr and Bolshakov [24, 25].

The reliability of each method was examined critically by creating a detailed uncertainty budget. Furthermore, FEM simulations helped assessing difficulties with tip positioning. Finally the report shows clearly potentials and limitations of the used techniques on a practically examined testing system. Moreover it gives recommendations how to prepare such a test on a thin solid film system and it identifies the parameters, which are important for getting reliable results.

2. Experimental details

The materials studied in this work are commercially available amorphous silicon nitride thin films deposited on silicon <100> from PLANO GmbH, Germany. Square openings were etched into the 200 µm thick silicon bulk material by the manufacturer in order to provide free standing membranes (Fig. 1a). These samples are available with different silicon nitride film thicknesses and opening dimensions. In this study 50 nm, 100 nm, 200 nm and 500 nm thick films (all nominal) were investigated. The membranes were spanned over 100 µm x 100 µm square openings.

2.1. Cantilever preparation

The above mentioned free-standing silicon nitride films were machined using a DualBeam Focused Ion Beam instrument FEI Quanta 3D FEG with Gallium source and an acceleration voltage of 30 kV. One-side clamped beams were milled at the edge of the openings (Fig.1b and 1c). The nominal width for all beams was adjusted to 2 µm. The beams for the 500 nm thick films had a nominal length of 15 µm and were machined with ion currents of 1 nA for rough milling and 50 pA for polishing the beam edges. The same was done for 200 nm thick films with a nominal beam length of 5 µm and rough milling at 0.3 nA, as well as for 100 nm and 50 nm thick films with a nominal length of 3 µm and rough milling ion currents of 0.1 nA and 50 pA respectively. For the subsequent bending test it was necessary to remove the rest of the free standing silicon nitride film in the opening using the ion beam. The exact length and width of the prepared beams were determined using the calibrated length measurement software within the FIB/SEM. The real thicknesses of the silicon nitride films were determined at one location of each specimen, at a site where the film was still adhering to the substrate, by preparing a cross-sectional sample by FIB technique and measure the silicon nitride layer thickness in a length scale calibrated TEM JEOL JEM 2200FS.

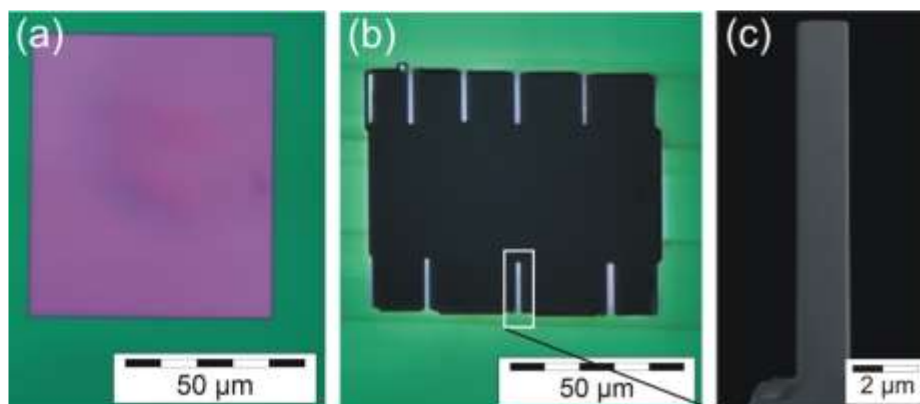

Fig.1 Sample: (a) light microscopic top-view image on a backside etched square with a free-standing silicon nitride film on top; (b) light microscopic image of FIB-prepared beams in the opening; (c) SEM-image of a silicon nitride beam ready for testing.

2.2. Micromechanical testing

The as-prepared beams were bent with a Force-Measurement-System (FMS) from Kleindiek Nanotechnik, Germany. This system is an extension tool for a micromanipulator from the mentioned supplier (Fig. 2a). The tool is equipped with a 400 µm long silicon cantilever, coated with a piezo-resistive material. In contact with another material it gives a voltage signal. The FMS is mounted in the vacuum chamber of the DualBeam machine. Every step can be observed by scanning electron microscopy.

Before starting to measure on the silicon nitride beams, the system has to be calibrated. Therefore a certified calibration spring from the German National Metrology Institute (PTB) with known spring constant (k_1) is displaced exactly 1 µm (Fig. 2b left). Together with the detected voltage a calibration value is calculated. All measured voltages are now multiplied by this calibration value and give the corresponding force value. To check whether this calibration value is plausible a second calibration spring with known spring constant k_2 (Fig. 2b right) is also displaced 1 µm. Then forces between 8 µN and 9, 8 µN are measured, which indicates a standard deviation for the force measurement of about 10 %.

A second parameter had to be checked before starting measurements, the stiffness of the used cantilever. During the test, bending of the cantilever should not take place. Therefore a maximum loading force for the FMS was determined experimentally. A calibrated microelectromechanical system (MEMS) device from PTB with a moveable main shaft was displaced about 6 µm (Fig. 2c). The stiffness of the MEMS is stable until a maximum displacement of 8 µm. When comparing both the theoretical and the measured force-displacement curves it becomes obvious that the slope (stiffness) is equal until a maximum force of about 7 µN. With higher forces the slopes differ more and more, which indicates that the cantilever of the FMS is bent.

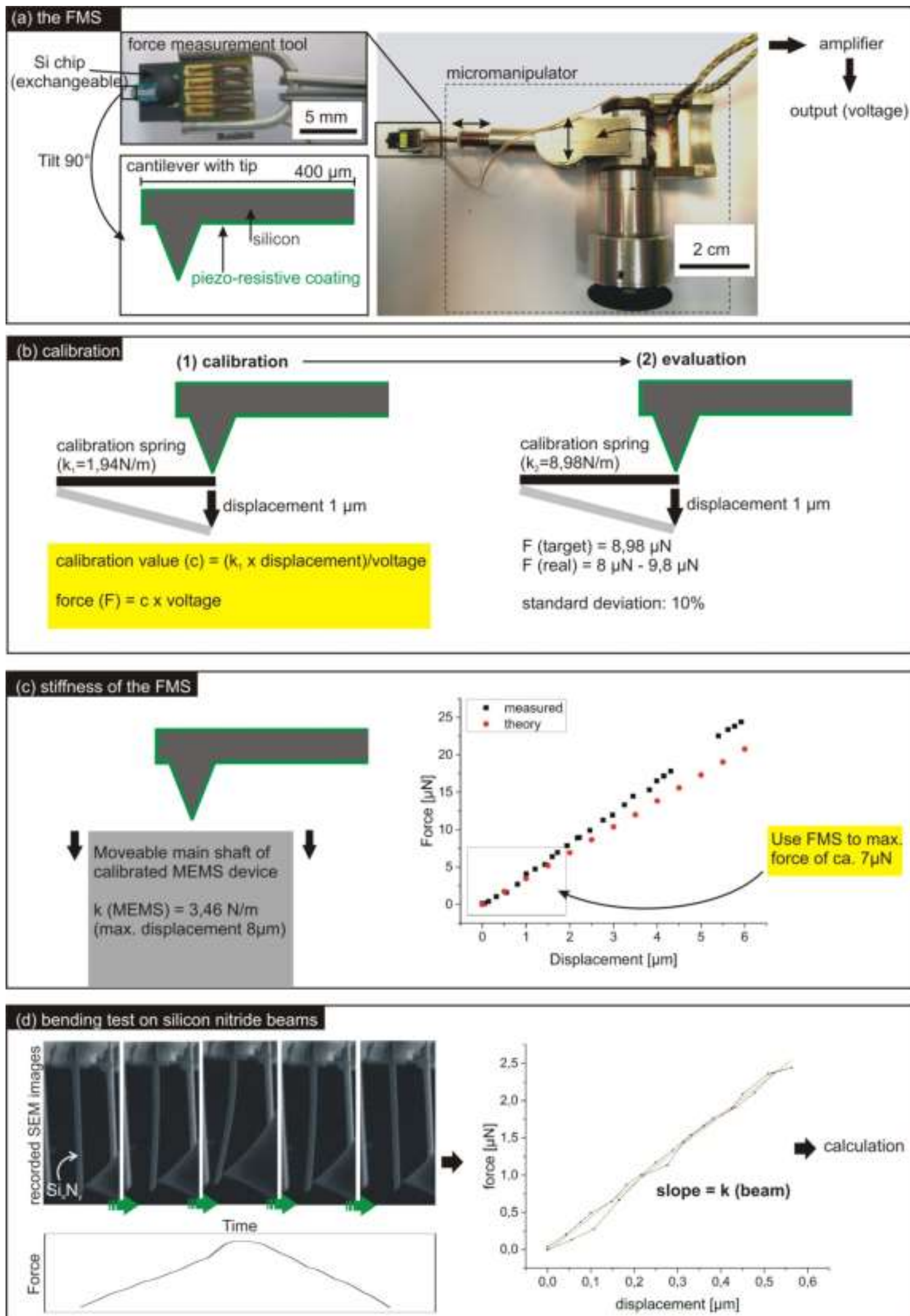

Fig. 2 (a) FMS setup and measuring principle; (b) calibration procedure; (c) checking the stiffness of the system with a calibrated MEMS; (d) silicon nitride beam bending experiment (Further information in the text).

The silicon nitride beams can be tested now (Fig. 2d). Unfortunately the system offers no automatic solution to apply constant forces or loading rates. Thus the beams were bent manually via driving knobs moving the micromanipulator in the three axes. However, preliminary tests showed that the manual bending with different bending speeds did not influence the resulting value significantly. The measured forces had to be correlated with the corresponding displacements. The displacements were measured with the image correlation software VEDDAC from Chemnitzer Werkstoffmechanik GmbH [26] applied to a series of images taken every second during the bending test by the SEM.

2.3 Instrumented Indentation Testing

The silicon nitride layers on the silicon substrate next to the openings with the free-standing membrane were characterized additionally by instrumented indentation technique using the XP head of the G200 Nano Indenter from Keysight Technologies. All measurements were carried out with a new Berkovich tip (three sided pyramid) with a nominal tip radius of 200 nm. To hold the temperature constant, the whole G200 system is inside a cabinet, where the current internal temperature is constantly measured and actively controlled. During the tests, the internal temperature was (21.1±0.1) °C.

For each of the four samples three maximum displacements h_{max} were chosen, which were less than or equal to the film thickness (please see displacement / film thickness rations in Fig. 4). The loading to h_{max} was controlled by keeping the loading rate divided by the load on the test surface constant at 0.05/s. The loading segment was followed by a short hold period of 10 s to reduce the possible influence of creep. A quick unload was done to 10 % of the maximum force F_{max}, with an unload rate of F_{max}*0.05/s, followed by a second hold period of 75 s for the determination of the thermal drift. Only the last 50 seconds were used to determine the

thermal drift by using a linear fit of the hold period data. The calculated correction of the thermal drift was normally between -0.05 nm/s and +0.05 nm/s. For each sample and chosen maximum displacement an array of 4x2 single indentation tests were performed. The distance between each indent was 25 µm in x- and y-direction.

Another important point was the determination of the exact (real) area function of the Berkovich tip, which was measured with fused silica as a reference material from the supplier of the nanoindenter system, assuming a depth independent Young's Modulus of 72 GPa and a Poisson's ratio of 0.17. Fifteen continuous stiffness measurement (CSM) indentation tests were performed. Here the contact stiffness is measured continuously as a function of indentation depth or frequency. In the new ISO 14577 [27], the usage of a variable epsilon and the correction of radial displacement are recommended for the calculation of the area function of the tip. Taking these corrections into account, Choduba and Jennet have shown that an area function can be calculated which agrees with the independent direct measurement such as traceably calibrated AFM [28]. Therefore the software Indent Analyser2 from ASMEC, which already contains these corrections, was used to calculate the square root of the contact area as a function of the contact depth h_c (fit function with five coefficients):

$$\sqrt{A_c} = c_1 + c_2 {h_c}^{1/4} + c_3 {h_c}^{1/2} + c_4 h_c + c_5 {h_c}^{3/2} \quad (1)$$

In this way a very accurate area function of the Berkovich tip could be obtained.

3. Results

3.1. Beam testing with the FMS

The real thicknesses of the silicon nitride layers on silicon were determined by TEM. In case of the 100 nm thick film the thickness of the film in an opening was checked additionally. This was necessary in order to check whether etching of the opening eventually has affected

film thickness. The results clearly showed that this was not the case. The TEM images and corresponding thickness values can be found in Figure 3 and Table1, respectively.

Seven tests were done per thickness with seven beams of similar dimensions. The detected force signal of the FMS software and the measured displacement were correlated for each bending test. The resulting curve was fitted linearly and a stiffness value k (the slope of the curve) for the tested object was obtained. With the exactly measured geometry of each beam a Young´s Modulus can be calculated according to the Euler-Bernoulli equation:

$$E = \frac{L^3}{3 \cdot I} \cdot k = \frac{4 \cdot L^3}{W \cdot T^3} \cdot k \qquad (2)$$

with the effective length L, area moment of inertia I, width W, thickness T and beam stiffness k. Here a rectangular cross-section is used. Figure 3b shows all calculated Young´s Moduli in overview. The uncertainty budget is discussed in detail in part 4. For the nominally 100 nm, 200 nm and 500 nm thick beams the values are more or less stable. In contrast the Young´s Moduli for the 50 nm thick beams scatter in a large range. This may be due to the fact, that these beams were twisted or bent after cutting with the FIB. Thus the silicon nitride membrane was under stress before, which was released during FIB machining. Therefore the 50 nm thick films will be neglected in the following discussion. The obtained Young´s Moduli are listed in Table 1.

In the literature lots of different values can be found for thin film amorphous silicon nitride: 210 GPa – 350 GPa for 100 nm - 500 nm thin beams measured by resonance spectra [29], 100 GPa – 300 GPa for 200 nm thin films deposited by various techniques [30], measured with IIT, and about 250 GPa for 160 nm thick film using bulge testing [31]. The calculated values in this study fit into the range given by the literature. Nevertheless, we wanted to check the reliability of our test results and therefore applied IIT as second independent method for the determination of the Young´s Modulus.

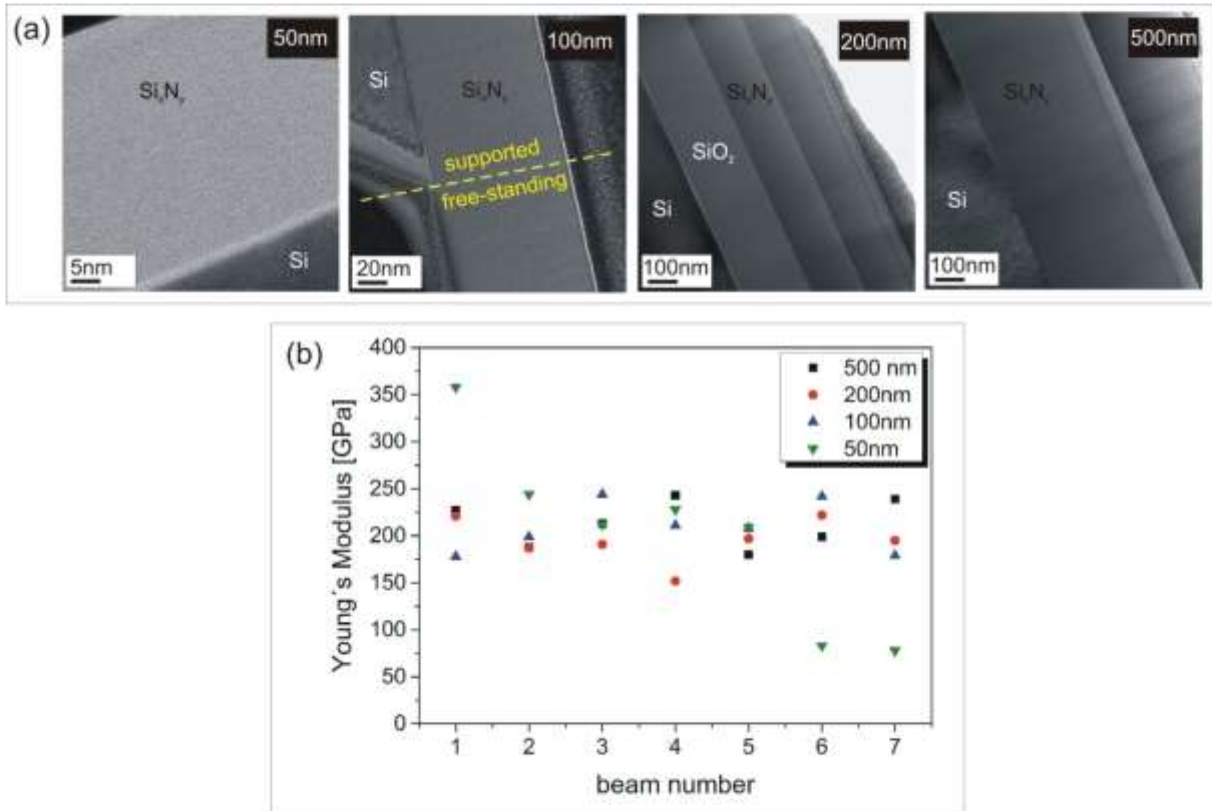

Fig. 3: (a) cross-sectional TEM images of the amorphous silicon nitride films (not indicated layers are deposited platinum films protecting the surface during FIB machining); (b) measured Young´s Moduli for nominally 50 nm, 100 nm, 200 nm and 500 nm thick silicon nitride beams.

Table 1 TEM measured thicknesses and mean Young´s Moduli obtained by the FMS method

Nominal thickness [nm]	TEM measured thickness [nm]	Young´s Modulus mean value [GPa]
50	50 ± 1,5	(202 ± 70)
100	97 ± 3	209 ± 24
200	182 ± 5,5	195 ± 22
500	515 ± 15,5	213 ± 25

3.2. Thin film testing with IIT

The evaluation of the measured data from the quasi static indentation tests on all four samples is divided into two steps.

In the first step, the data were analysed according to the method of Oliver and Pharr (O.& P.) [32]. Hereby the correction of the radial displacement and the variable epsilon was taken into account by using the software Indent Analyser2. It was necessary to export the data including the thermal drift correction (force, displacement and time) of each single load-displacement curve from the G200 control program NanoSuite6 to the Indent Analyser2 program. Then each curve was corrected for the zero-point before analysing them to calculate the indentation modulus and the contact radius at maximum force. Finally an effective indentation modulus is obtained, which can be brought into relation to the classic defined Young´s Modulus taking into mind that both values are not completely the same. Figure 4a shows the evaluated mean effective indentation modulus, still affected by the influence of the silicon substrate, plotted over the ratio of displacement to film thickness. This was done for all eight curves for each displacement and tested sample. As shown in the diagram the effective indentation modulus decreases with increasing displacement for the 500 nm, 200 nm and 100 nm silicon nitride films. That indicates that the stiffness of the film is much higher than the substrate and consequently the Young's Moduli for these three films must be higher. Noteworthy here is the different behaviour in the case of the 200 nm thin silicon nitride film. The overall lower effective indentation moduli in comparison to the 100 nm and 500 nm thin films can be explained by the influence of the much less rigid silicon dioxide interlayer (see also Fig. 3a). This indicates that all obtained indentation moduli – even for very small indentation depths – are affected by the substrate influence and thus a simple extrapolation of the effective indentation modulus to the displacement/thickness ratio = 0 won´t lead to reliable Young's moduli for the silicon nitride films since we do not expect completely different mechanical behaviour between the certain film thicknesses. In the case of the 50 nm silicon nitride film an increase of the effective indentation modulus with higher displacement was determined,

which could mean that here the Young's Modulus of the silicon nitride film is lower than the one of the silicon substrate. Since this is not very likely, we rather assume an impact of residual stress within the coating. This interpretation is corroborated by the observation of beam twisting after FIB cutting, as described in 3.1.

The standard deviation is mostly between 2 GPa and 7 GPa. Only for the small depth measurement of the 100 nm silicon nitride (25 GPa), as well as for the 50 nm silicon nitride (15 GPa and 10 GPa) the standard deviation is much higher.

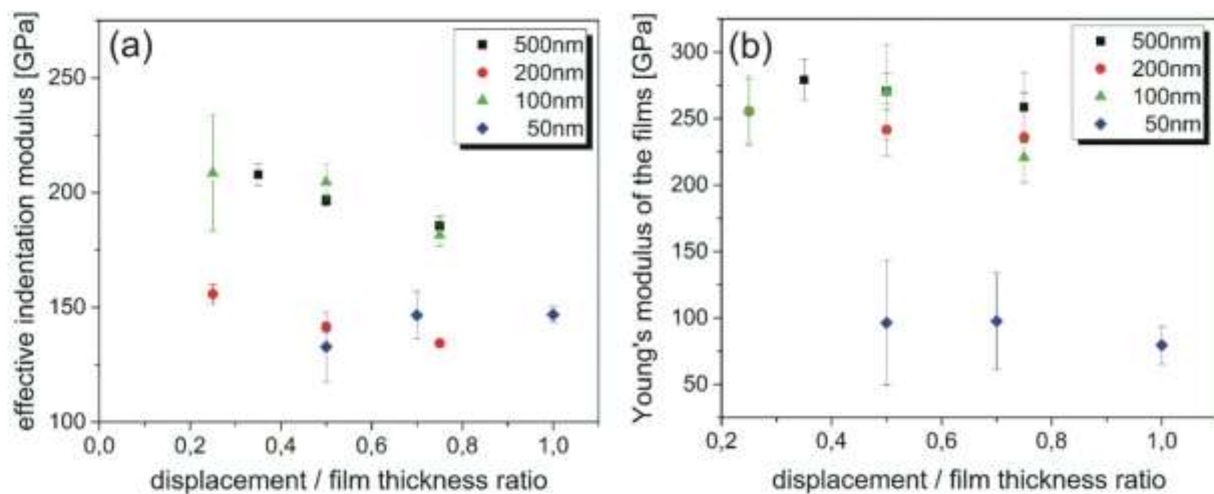

Fig. 4: (a) Effective indentation moduli for the nominally 50 nm, 100 nm, 200 nm and 500 nm thin silicon nitride films on a silicon substrate, calculated by the O.& P.-method; (b) Young's Moduli for the nominally 50 nm, 100 nm, 200 nm and 500 nm thin silicon nitride films on a silicon substrate without influence of the substrate calculated with the software ISA. (*Error values are only given for the statistical errors.)

To convert the substrate affected effective indentation moduli into unaffected Youngs`s Moduli the concept of the effective indenter shape was applied [24, 25], which is already implemented as an analysing tool into the software package ISA from SIOMEC. The main idea of this concept is to find an effective indenter which when loaded into a flat surface, gives for an elastic half-space the same displacement that would be given by the real used

indenter loaded into the tested material deformed by the plastic hardness impression. The effective indenter shape can be described by

$$z = Br^n \quad (3)$$

where B and n are material constants that depend on the distribution of pressure under the indenter and z and r are cylindrical coordinates. In simple terms, a plastic-elastic contact problem is transformed into a pure elastic one, which gives us the possibility to calculate a Young's Modulus from the unload-curve containing also the elastic material response of the substrate and other involved interlayer.

Therefore three different unload curves from the measured eight curves of each batch were chosen and saved after analysis with Indent Analyser2 as ASCII files. Those files contain the data for displacement, load and time. Together with the determined effective indentation modulus and the contact radius at maximum force, considering the correction of the radial displacement and the variable epsilon, the effective indenter was fitted from the unload-curve. The range of the unload-curve was fitted with 30 data points from 98% to 40%. After calculating the effective indenter, the parameters for the substrate and the films have been entered. These parameters are the Poisson ratios, the Young's Modulus for the substrate and other interlayer, as well as the exact value of the film and interlayer thicknesses. The parameters used in this work are shown in Table 2.

Table 2 Parameters used in ISA for the calculation of the Young's Modulus of the silicon nitride-films

Poisson ratios	Silicon nitride film	0,23
	SiO_2	0,18
	Si	0,262
Young's Modulus	SiO_2	70 GPa
	Si	169 GPa
Film thicknesses	Silicon nitride (500 nm nominal)	515 nm

	Silicon nitride (200 nm nominal)	182 nm (250 nm SiO_2 interlayer)
	Silicon nitride (100 nm nominal)	97 nm
	Silicon nitride (50 nm nominal)	50 nm
Fit parameters	Fit unload-curve	30 data points for fit
		40% - 98% fit range
	Fit accuracy	normal
	Fit speeding up calculation	highest accuracy

After calculating the effective indenter and the input of the material parameters, the calculation of the film Young's Modulus was done. The option for the "fit accuracy" was set to normal and for the "speeding up calculation" to highest accuracy, which shows to be a good compromise between accuracy of the fit and time of the computing. The described fit procedure was carried out for each curve according to the same principle and the results are shown in Figure 4b. In the cases of the 500 nm, 200 nm and 100 nm silicon nitride films an increase of the modulus can be found for each displacement/film thickness ratio compared to the results of the classic O. & P. evaluation. The calculated values for the Young's Modulus are in the range of (254 ± 19) GPa. The results for the 200 nm silicon nitride film fit much better to the rest, since the influence of the additional silicon dioxide interlayer is eliminated effectively. But also here the calculated mean values for the modulus aren't constant and a slight decrease can be observed with increasing indentation depth. In the case of the 50 nm silicon nitride film the calculated mean value for the modulus is with (91 ± 10) GPa much lower as from the classical O. & P. method. As discussed previously, such a low Young's Modulus for a silicon nitride film is unlikely.

Table 3 Young's Moduli for all four silicon nitride films, without the influence of the substrate (mean values of all displacement/thickness ratios per sample)

silicon nitride film	Young's Modulus

thickness (nominal) [nm]	[GPa]
50	91 ± 10
100	249 ± 25
200	244 ± 10
500	269 ± 10

4. Discussion

As shown in the previous part, both investigation techniques have their own difficulties to measure mechanical properties of thin film structures. To assess the reliability of the results it is paramount to have a critical look on the existing sources of error.

4.1. The FMS method – estimated uncertainty budget

The uncertainty for the force value can be set about 10 %. The measured displacement has to be considered with an error of about 1%. In most of the cases the tip and the surface of the tested beam were not exactly at 90°. The positioning of the tip was roughly done by hand before the whole equipment is evacuated in the SEM. The tip can´t be rotated, therefore it is possible that the cantilever tip is not exactly in 90° to the surface of the tested sample. Here the uncertainty of 1 % can be estimated additionally for the force value. All the mentioned errors influence mainly the stiffness k, which is directly proportional to the Young´s Modulus. Further uncertainties are the geometry parameters of the object, which have a much larger influence on the resulting value. First the uncertainty of the width and the length of the tested beam amounts to 3 % because of the possible error in SEM length scale measurement. The possibility that the tip slides some nanometers on the smooth beam surface during large

displacements - and therefore changes the effective length of the beam - was considered in the calculation of the Young´s Modulus in part 3. The thickness of the silicon nitride film was determined by TEM as exact as possible, because this parameter is multiplied by the negative third power in the Euler-Bernoulli equation. Nevertheless an uncertainty of 3 % has to be taken into account for the TEM thickness measurement.

An error propagation calculation can be done for all the termed sources of error and Table 4 shows the obtained values.

$$\Delta E = \sqrt{\left(\frac{4 \cdot L^3}{W \cdot T^3} \cdot \Delta k\right)^2 + \left(\frac{12 \cdot k \cdot L^2}{W \cdot T^3} \cdot \Delta L\right)^2 + \left(\frac{4 \cdot k \cdot L^3}{W^2 \cdot T^3} \cdot \Delta W\right)^2 + \left(\frac{12 \cdot k \cdot L^3}{W \cdot T^4} \cdot \Delta T\right)^2} \quad (4)$$

Table 4 Calculated uncertainty values for the Young´s Modulus

Thickness [nm] nominal	Young´s Modulus E [GPa] mean value	Standard deviation for the Young´s Modulus [GPa]	Uncertainty ±ΔE [GPa]
100 nm	209	24	21
200 nm	195	22	15
500 nm	213	25	20

There are some more errors which can influence the mechanical behavior and the result. The beams were machined with the help of Gallium-Ions. These ions are implanted in the material and thus may change the composition and mechanical properties within a superficial layer of the tested beam. In a former study we found out that this implantation depth can be set to maximum of 10 nm for 30 kV ion beam at the edges of the tested object, which is less than 1 % damaged volume of the whole object [33]. Thus the influence of the implanted ions can be neglected here as well as the presence of intrinsic stresses in the film which should be completely released by cutting free the membrane. An important evidence on intrinsic stress

is the buckling of the released structure [34], which was observed only in case of the 50 nm thin film. Not completely ruled out is that the ion beam machining slightly rounds the edges of the beam and an ideal rectangular shape is maybe not reached in all cases.

Usually the beam is bent at mid-width, but concerning the instrumentation setup it is difficult to hit the exact mid-width position. To estimate this uncertainty, force-displacement-curves were simulated by FEM with bending 10% and 50% next to the mid-width position of a 2 µm wide, 5 µm long and 100 nm thin beam. The resulting slope k was just -0.06 % and -1.64 % different from the calculated k at exact mid-width bending. Thus hitting the exact mid-width is not a prerequisite for obtaining reliable results.

Finally to complete the list of uncertainties both the elastic-plastic deformation of the FMS tip and the thermal drift has to be taken into account. These errors should be very small, because the tested objects are quite soft compared to the tip and the FIB/SEM room was under climate control.

4.2. Indentation testing

4.2.1. Experimental data and O. & P. - evaluation with Indent Analyser2

Due to the complex nature of the plastic-elastic material behavior during the nanoindentation a lot of factors have an influence on the result of the measured and calculated Young's Modulus, especially for thin films. All of the quasi-static indentation experiments were carried out related to the ISO standard 14577 and also taking into account the correction for the radial displacement and the variable epsilon. The load-displacement curves for each batch show a distinct scattering. It was investigated, that the poor repeatability depends mainly on the drift correction, which was on average about ± 0.05 nm/s, but because of the very small penetration depth, the drift correction, even for these small values, shifts the curves by several nanometers along the displacement axis. The high standard deviation of the effective

indentation modulus calculated with the O. & P. -method can be explained by such a poor repeatability. A better control of the environment or a more sophisticated method of determining the drift correction could lead to a better repeatability. However, it cannot be ruled out that also inhomogeneity of the material, intrinsic stresses, determination of the zero point, film thickness variations as well as surface roughness have an influence on the measured scattering of the load-displacement curves, because of the high local resolution of the nanoindentation method.

4.2.2. Calculation of the film Young's Modulus with ISA

ISA gives the operator the possibility to calculate the Young's Modulus of a film without the influence of the substrate. Therefore it is necessary to know exactly the right area function of the tip which was used in the test or at least the right contact radius at maximum load. During the calculation and fitting process it was found out that even a small variation of the contact radius by 1 % leads to a change of maximum 5 % for the Young's Modulus. Another important influence on the calculated results is the knowledge of the exact film thickness. In Table 5 this influence is shown for the results of the modulus for one measurement on the 100 nm silicon nitride film. An uncertainty of 3 % for the film thickness results in a variation of 1 % for the calculated Young's Modulus.

Table 5 Influences of the film thickness on the results of the calculated Young's Modulus (Taking into account an uncertainty of 3 % for the measured film thickness by TEM)

Sample	Film thickness [nm]	Young's Modulus [GPa]
Silicon nitride (100 nm)	97 (measured by TEM)	267
(displacement/film thickness	100 (+3%)	264
ratio 0.5)	95 (-3%)	269

In consideration of the discussed systematic errors and uncertainties, the results of the Young's Moduli calculated with ISA show a good agreement with the made assumptions, that the Young's Modulus for the 500 nm, 200 nm and 100 nm silicon nitride film is need to be higher than the effective indentation moduli from the classic evaluation (O. &. P.). In the case of the 50 nm silicon nitride film the assumption was that the Young's Modulus without the influence of the substrate should be lower than the effective indentation modulus, what was also found with ISA. The high gap in the Young's Moduli between the 50 nm film und the other silicon nitride films cannot be satisfactorily clarified, but we assume that intrinsic stresses play a mandatory role here. Nevertheless the ISA software is tool assuming ideal testing conditions. That means real effects like intrinsic stresses, inhomogeneities, roughness, interface conditions, the exact knowledge of the shape of the indenter or other influences aren't taken into account or can just estimated and lead to a high standard deviation.

4.3. Conclusions on the comparability of the methods

Both methods provide plausible results with a sufficient reproducibility and a part of the values can be found in an intersecting set. Nevertheless a small deviance between the results of both methods persists. But in relation to the diversity of uncertainties and sources of error a deviance between both is a more realistic scenario than a complete match of the results. Especially noteworthy in the list of uncertainties are: The exact knowledge of film thickness on the particular tested region, beam length, and area function of the intender tip, which influence the result enormously. A small deviance here shifts the Young´s Modulus tens of GPa in one direction and will lead to more or less fitting of results. The determination of these parameters implies a great experimental effort. Especially for the geometry parameters in the sub-micron and nano range TEM work is necessary.

Moreover it can´t be ruled out that the free-standing silicon nitride is slightly different in composition due to etching process to create an opening in the silicon wafer [29]. Intrinsic stresses in the adhered films on the bulk silicon can also influence the result, despite the fact that visible stress was only observed in case of the 50 nm thin silicon nitride film [35].

Finally the methods based on two completely different models implying a lot of assumptions and simplifications especially when the film thickness tends to the nanoscale. Originally the determination of the Young´s Modulus was realized by tensile testing and plotting stress-strain curves, where the Young´s Modulus represents the initial linear slope. To make sure that tests are comparable one have to know the exact sample geometry and the same conditions for testing have to be realized since the Young´s Modulus depends on the temperature, humidity and strain rate. Going over to the nanoindentation a direct measurement of the Young´s Modulus is not possible. An indentation modulus is measured, which has generally speaking the same meaning as the Young´s Modulus, but the stiffness behavior is just measured locally under three-axis load. This leads to a difference in terms of the value. In the end the indentation modulus can´t be raised for the purpose of dimensioning. In contrast the bending test as a conventional method especially for brittle materials provides theoretically more explicit values. But also here are some difficulties. The Euler-Bernoulli equation as described in the text is actually valid only for small displacements. That means the displacement has to be much smaller than the thickness of the testing sample. This could not be realized within our testing set-up, because such small displacements can´t be resolved accurately with the scanning electron microscope yet. With large displacements sliding phenomena occur as described in 4.1. The solution of this problem probably lies in advanced theories like the micropolar theory [36]. Additionally the models of both techniques are originally developed for testing at least for micro and macro samples. In this study the same were applied for testing at the nanoscale as well.

In the final conclusion neither the FMS method nor the nanoindentation can generate a “true value”. Absolute values are just comparable within the same method executing exact the same experimental procedure. Ruling out the measurements with the 50 nm thick membranes because of difficulties with residual stresses, the relative trends observed with both methods are in good agreement. Thus a size effect for the Young´s Modulus could not be observed in both studies, at least down to a thickness of 100 nm.

Acknowledgement

This research is supported by the European Union by funding the European Metrology Research Programme (EMRP) project “Traceable measurement of mechanical properties of nano-objects (MechProNO)”. The EMRP is jointly funded by the EMRP participating countries within EURAMET and the European Union. The authors like to thank PTB for providing calibrated springs and MEMS. Especially Sai Gao (PTB) is gratefully thanked for the FEM simulations and Ilona Dörfel (BAM) as well as Ines Häusler (BAM) for the TEM work.

References

[1] X. Zhang, C. Duan, L. Liu, X. Li, H. Xie, A non-resonant fiber scanner based on an electrothermally-actuated MEMS stage, Sensor. Actuat. A-Phys. 233 (2015) 239-245.

[2] S. Fanget, F. Casset, R. Dejaeger, F. Maire, B. Desloges, J. Deutzer, R. Morisson, Y. Bohard, B. Laroche, J. Escato, Q. Leclere, Low voltage MEMS digital loudspeaker array based on thin-film PZT actuators, Physics Procedia. 70 (2015) 983-986.

[3] T. A. Emadi, D. A. Buchanan, A novel 6x6 element MEMS capacitive ultrasonic transducer with multiple moving membranes for high performance imaging applications, Sensor. Actuat. A-Phys. 222 (2015) 309-313.

[4] Z. Qiu, W. Piyawattanametha, MEMS based fiber optical microendoscopes, Displays. 37 (2015) 41-53.

[5] J. Karchňák, D. Šimšik, B. Jobbágy, A. Galajdová, D. Onofrejová, MEMS sensors in evaluation of human biomechanical parameters, Procedia Engineering. 96 (2014) 209-214.

[6] W.-E. Fu, Y.-Q. Chang, C.-W. Chang, C.-K. Yao. J.-D. Liao, Mechanical properties of ultra-thin HfO_2 films studied by nano scratches tests, Thin Solid Films, 529 (2013) 402-406.

[7] M. A. Hassan, A. R. Bushora, R. Mahmoodian, Identification of critical load for scratch adhesion strength of nitride-based thin films using wavelet analysis and a proposed analytical model, Surf. Coat. Tech. 2077 (2015) 216-221.

[8] Y. Liu, C.-F. Guo, S. Huang, T. Sun, Y. Wang, Z. Ren, A new method for fabricating ultrathin metal films as scratch-resistant flexible transparent electrodes, Journal of Materiomics 1 (2015) 52-59.

[9] S. Roy, E. Darque-Ceretti, E. Felder, F. Raynal, I. Bispo, Experimental analysis and finite element modeling of nano-scratch test applied on 40- 120 nm SiCN thin films deposited on Cu/Si substrate, Thin Solid Films. 518 (2010) 3859-3865.

[10] S. Sundararajan, B. Bhushan, Development of AFM-based techniques to measure mechanical properties of nanoscale structures, Sensor. Actuat. A-Phys. 101 (2002) 338-351.

[11] T. Fritz, M. Griepentrog, W. Mokwa, U. Schnakenberg, Determination of Young´s Modulus of electroplated nickel, Electrochim. Acta. 48 (2003) 3029-3035.

[12] M. Griepentrog, G. Krämer, B. Cappella, Comparison of nanoindentation and AFM methods for the determination of mechanical properties of polymers, Polym. Test. 32 (2013) 455-460.

[13] M.-J. Pac, S. Giljean, C. Rousselot, F. Richard, P. Delobelle, Microstrucural and elasto-plastic material parameters identification by inverse finite elements method of $Ti_{(1-x)}Al_xN$ ($0<x<1$) sputtered thin films from Berkovich nano-indentation experiments, Thin Solid Films. 569 (2014) 81-92.

[14] E. P. S. Tan, C. T. Lim, Mechanical characterization of nanofibers – A review, Compos. Sci. Technol. 66 (2006) 1102-1111.

[15] M. J. Gordon, T. Barron, F. Dhalluin, P. Gentile, P. Ferret, Size effects in mechanical deformation and fracture of cantilevered silicon nanowires, Nano Lett. 9 (2009) 525-529.

[16] F. Iqbal, J. Ast, M. Göken, K. Durst, In situ micro-cantilever tests to study fracture properties of NiAl single crystals, Acta Mater. 60 (2012) 1193-1200.

[17] M. Palacio, B. Bhushan, N. Ferrell, D. Hansford, Nanomechanical characterization of polymer beam structures for BioMEMS applications, Sensor. Actuat. A-Phys. 135 (2007) 637-650.

[18] B. N. Jaya, C. Kirchlechner, G. Dehm, Can microscale fracture tests provide reliable fracture toughness values? A case study in silicon, J. Mater. Res. 30 (2015) 686-689.

[19] M. Trueba, D. Gonzales, J. M. Martínez-Esnaola, M. T. Hernandez, D. Pantuso, H. Li, I. Ocaña, M R. Elizalde, Fracture characterization of brittle thin-film membrane testing, Thin Solid Films. 564 (2014) 314-320.

[20] M. Trueba, D. Gonzalez, M. R. Elizalde, J. M. Martínez-Esnaola, M. T. Hernandez, H. Li, D. Pantuso, I. Ocaña, Assessment of mechanical properties of metallic thin-film through micro-beam testing, Thin Solid Films. 571 (2014) 296-301.

[21] C. C. Lee, G. Alici, G. M. Spinks, G. Proust, J. M. Cairney, Micron-scale polymer-metal cantilever actuators fabricated by focused ion beam, Sensor. Actuat. A-Phys. 172 (2011) 462-470.

[22] A.K. Bhattacharya, W.D. Nix, Analysis of elastic and plastic deformation associated with indentation testing of thin films on substrates, Int. J. Solids Struct. 24 (1988) 1287-1298.

[23] T. Chudoba, M. Griepentrog, A. Dück, D. Schneider, F. Richter, Young's modulus measurements on ultra-thin coatings, J. Mater. Res. Vol.19. (2004) 301-314

[24] G.M. Pharr, A. Bolshakov, Understanding nanoindentation unloading curves, J. Mater. Res. Vol.17 (2002) 2660-2671

[25] J. Woirgrad , J.C. Dargenton, An alternative method for penetration depth determination in nanoindentation measurements, J. Mater. Res. Vol.12 (1997) 2455-2458

[26] http://www.cwm-chemnitz.de/produkte/software, processed in 2013, viewed in Oct. 2015.

[27] ISO 14577 Metallic materials-Instrumented indentation test for hardness and materials parameters, ISO Central Secretariat, Geneva, Switzerland, part 1 - 3 (2015), part 4 (2007)

[28] T. Chudoba, N.M. Jennet, Higher accuracy analysis of instrumented indentation data obtained with pointed indenters, J. Phys. D: Appl. Phys. Vol. 41 (2008) 215407 (16pp)

[29] K. Babaei Gavan, H. J. R. Westra, E. W. J. M. Van der Drift, W. J. Venstra, H. S. J. Van der Zant, Impact of fabrication technology on flexural resonances of silicon nitride cantilevers, Microelectron. Eng. 86 (2009) 1216-1218.

[30] P. Morin, G. Raymond, D, Benoit, P. Maury, R. Beneyton, A comparison of the mechanical stability of silicon nitride films deposited with various techniques, Appl. Surf. Sci. 260 (2012) 69-72.

[31] Y. Hwangbo, J.-M. Park, W. L. Brown, J.-H. Goo, H.-J. Lee, S. Hyun, Effect of deposition conditions on thermo-mechanical properties of free standing silicon-rich silicon nitride thin film, Microelectron. Eng. 95 (2012) 34-41.

[32] W.C. Oliver, G.M. Pharr, An improved technique for determining hardness and elastic modulus using load and displacement sensing indentation experiments, J. Mater. Res. Vol.7 (1992) 1564-1583

[33] N. Wollschläger, W. Österle, I. Häusler, M. Stewart, Ga^+ implantation in a PZT film during focused ion beam micro-machining, Phys. Status Solidi C, 12 (2015) 314-317.

[34] G. Pennelli, M. Totaro, A. Nannini, Correlation between surface stress and apparent Young´s Modulus of top-down silicon nanowires, ACS Nano 6 (2012) 10727-10734.

[35] J. He, C. M. Lilley, Surface stress effect on bending resonance of nanowires with different boundary conditions, Appl. Phys. Lett. 93 (2008) 263108-1-3.

[36] A. W. McFarland, J. S. Colton, Role of material microstructure in plate stiffness with relevance to microcantilever sensors, J. Micromech. Microeng. 15 (2005) 1060-1067.